MicroRNA-21/PDCD4 Proapoptotic Signaling From Circulating CD34$^+$ Cells to Vascular Endothelial Cells: A Potential Contributor to Adverse Cardiovascular Outcomes in Patients With Critical Limb Ischemia

Gaia Spinetti,[1] Elena Sangalli,[1] Elena Tagliabue,[1] Davide Maselli,[1] Ornella Colpani,[1] David Ferland-McCollough,[2] Franco Carnelli,[1] Patrizia Orlando,[1] Agostino Paccagnella,[3] Anna Furlan,[3] Piero Maria Stefani,[3] Luisa Sambado,[3] Maria Sambataro,[3] and Paolo Madeddu[2]

Diabetes Care 2020;43:1520–1529 | https://doi.org/10.2337/dc19-2227

OBJECTIVE

In patients with type 2 diabetes (T2D) and critical limb ischemia (CLI), migration of circulating CD34$^+$ cells predicted cardiovascular mortality at 18 months after revascularization. This study aimed to provide long-term validation and mechanistic understanding of the biomarker.

RESEARCH DESIGN AND METHODS

The association between CD34$^+$ cell migration and cardiovascular mortality was reassessed at 6 years after revascularization. In a new series of T2D-CLI and control subjects, immuno-sorted bone marrow CD34$^+$ cells were profiled for miRNA expression and assessed for apoptosis and angiogenesis activity. The differentially regulated miRNA-21 and its proapoptotic target, PDCD4, were titrated to verify their contribution in transferring damaging signals from CD34$^+$ cells to endothelial cells.

RESULTS

Multivariable regression analysis confirmed that CD34$^+$ cell migration forecasts long-term cardiovascular mortality. CD34$^+$ cells from T2D-CLI patients were more apoptotic and less proangiogenic than those from control subjects and featured miRNA-21 downregulation, modulation of several long noncoding RNAs acting as miRNA-21 sponges, and upregulation of the miRNA-21 proapoptotic target PDCD4. Silencing miR-21 in control CD34$^+$ cells phenocopied the T2D-CLI cell behavior. In coculture, T2D-CLI CD34$^+$ cells imprinted naive endothelial cells, increasing apoptosis, reducing network formation, and modulating the TUG1 sponge/miRNA-21/PDCD4 axis. Silencing PDCD4 or scavenging reactive oxygen species protected endothelial cells from the negative influence of T2D-CLI CD34$^+$ cells.

CONCLUSIONS

Migration of CD34$^+$ cells predicts long-term cardiovascular mortality in T2D-CLI patients. An altered paracrine signaling conveys antiangiogenic and proapoptotic features from CD34$^+$ cells to the endothelium. This damaging interaction may increase the risk for life-threatening complications.

[1]IRCCS MultiMedica, Milan, Italy
[2]University of Bristol, Bristol, U.K.
[3]Ca Foncello Hospital, Treviso, Italy

Corresponding author: Gaia Spinetti, gaia.spinetti@multimedica.it, or Paolo Madeddu, mdprm@bristol.ac.uk

Received 5 November 2019 and accepted 30 March 2020

This article contains supplementary material online at https://doi.org/10.2337/figshare.12075639.

The chemokine stromal-derived factor 1 (SDF-1) participates in cardiovascular repair through the mobilization of bone marrow (BM)-derived $CD34^+$ progenitor cells that express the CXCR4 receptor. $CD34^+CXCR4^+$ cells positively interact with the vascular endothelium by releasing trophic soluble factors and extracellular vesicles (EVs). Risk factors, ageing, and age-related diseases compromise this homeostatic mechanism by perturbing the BM microenvironment (1,2). Interestingly, both biased myelopoiesis and deficit/dysfunction of $CD34^+$ cells are associated with an increased risk of cardiovascular morbidity and mortality (3–10).

We showed that $CD34^+$ cell migration predicted cardiovascular mortality in patients with type 2 diabetes (T2D) undergoing revascularization of critical limb ischemia (CLI) (10). Phenotypic changes in $CD34^+$ cells may cause systemic vascular damage in these high-risk patients through antiangiogenic and proapoptotic miRNAs (miRs) (10–13).

The current study investigated *1*) if $CD34^+$ cells predict cardiovascular mortality long term and *2*) how $CD34^+$ cells cause vascular damage instead of repair.

RESEARCH DESIGN AND METHODS

See Supplementary Material online for supplementary tables and figures.

Study 1: $CD34^+$ Cell Migration Predicts Long-term Mortality

We performed a phone survey of T2D-CLI patients recruited in the NCT01269580 study, which demonstrated that migration of peripheral blood (PB) $CD45^{dim}CD34^+CXCR4^+KDR^+$ cells predicted cardiovascular death after angioplasty (10). At 6 years, 15 patients were lost to follow-up and were therefore excluded. Baseline characteristics of the remaining 104 patients are summarized in Supplementary Table 1.

Study 2: Molecular Mediators of $CD34^+$ Cell–Induced Vascular Damage

Clinical characteristics of a new cohort comprising 47 control subjects and 41 patients with T2D, of which 30 affected by CLI, are reported in Supplementary Table 2. T2D and CLI were defined according to the American Diabetes Association and TASC 2007, respectively. Exclusion criteria: acute disease/infection, immune diseases, current/past hematological disorders or malignancy, unstable angina, recent (within 6 months) myocardial infarction or stroke, liver failure, renal failure, and pregnancy. All participants signed an informed consent to donate the BM leftovers from the femoral head otherwise discarded during hip replacement surgery (control subjects and subjects with T2D without complications) or BM aspirates of the iliac crest performed ad hoc for the study (patients with T2D-CLI).

The studies received ethical authorization from the IRCCS MultiMedica (PROT 20/2010), Bristol University (REC14/SW/1083 and REC14/WA/1005), and Santa Maria Ca' Foncello Hospital (DDG 2333/2017) (13,14). BM-$CD34^+$ cells were assessed in situ or following immunomagnetic bead isolation as previously described (13). Some assays were conducted using the $CD34^+$ cell–derived conditioned medium (CCM) and respective EVs collected using Exospin kit (Cell Guidance System) following the manufacturer's instructions.

miR and Gene Expression Analyses of $CD34^+$ Cells

miR profiling was conducted at Exiqon Services, Vedbæk, Denmark. Total RNA (30 ng) was reverse-transcribed using the miRCURY LNA Universal reverse transcriptase (RT) miR PCR, Polyadenylation and cDNA synthesis kit (Exiqon). The amplification was performed in a LightCycler 480 Real-Time PCR System (Roche) in 384-well plates. A total number of 372 miRs were tested. A cut-off ($C_t > 37$) was used to consider a miR as expressed and included in the subsequent analyses.

For biological validation and expressional studies, RNA was extracted from cultured cells, cell-derived CCM/EVs, plasma, and plasma-derived EVs using miRNeasy Mini Kit (Qiagen) following the manufacturer's instructions. Quantitative RT-PCR was performed with the QuantStudio 6 Flex Real-Time PCR using miR TaqMan probes (Thermo Fisher) and long noncoding RNA (ncRNA)/gene primers listed in Supplementary Table 3. miR-21 was silenced in control BM-$CD34^+$ cells by transfecting them with 50 nmol/L anti-miR-21–5p (AM10206; Ambion), while controls were transfected with a nontargeting sequence or scramble (SCR) (AM4611, Silencer Negative Control; Ambion), using transfection reagents (Genlantis) according to the manufacturer's protocol.

In Vitro Migration and Flow Cytometry

PB–mononuclear cell (MNC) in vitro migration assays using SDF-1 as a chemoattractant were performed using transwell chambers as described (10). Migrated cells were stained for surface antigens CD45 (FITC; BD Biosciences), CD34 (PeCy7; BD Biosciences), and CXCR4 (APC; BD Biosciences), then fixed in Met-OH, permeabilized in PBS-Tween 0.1%-BSA 0.5%, and stained for intracellular antigen PDCD4 (Abcam) with secondary antibody anti-rabbit-phycoerythrin (BD Biosciences). Cells were analyzed using a FACSCanto flow cytometer with the FACSDiva software (both from BD Biosciences).

Apoptosis Assay

BM-$CD34^+$ cells or human umbilical vascular endothelial cells (HUVECs) were stained with 7-aminoactinomycin D (7-AAD)/Annexin-V and analyzed on FACSCanto II flow cytometer (BD Biosciences). The $7\text{-}AAD^-$/Annexin V^+ combination identified apoptotic cells. Caspase-3/7 Assay (Promega) was performed on HUVECs exposed to $CD34^+$ cells CCMs.

PDCD4 Silencing

HUVECs were transfected with 50 nmol/L siPDCD4 (Dharmacon) or nontargeting sequence (AM4611, Silencer Negative Control; Ambion).

Immunostaining

Immunofluorescence. Paraffin-embedded BM sections were incubated with the following: rabbit anti-PDCD4 (1:200; abcam), mouse anti-CD34 (1:5; Dako), and rabbit anti-4-hydroxy-2-nonenal (4-HNE) (1:500; Bioss). Nuclei were counterstained with DAPI (1 μg/mL) (Sigma-Aldrich). Images were acquired with a fluorescent microscope (DM6 B; Leica Microsystems) at 63× magnification and analyzed using Fiji software. Cultured HUVECs were fixed with 4% paraformaldehyde (PFA) (Electron Microscopy Science), permeabilized with 0.3% triton (Sigma-Aldrich), and stained with rabbit anti-PDCD4 (1:200). Nuclei were counterstained with DAPI (1 μg/mL) (Sigma-Aldrich). Microphotographs were captured using a Zeiss microscope equipped with digital image processing software (AxioVision Imaging System).

Immunohistochemistry. BM sections were stained with rabbit anti-PDCD4 (1:200) by BenchMark ULTRA system (Roche). Ten images for each sample were acquired

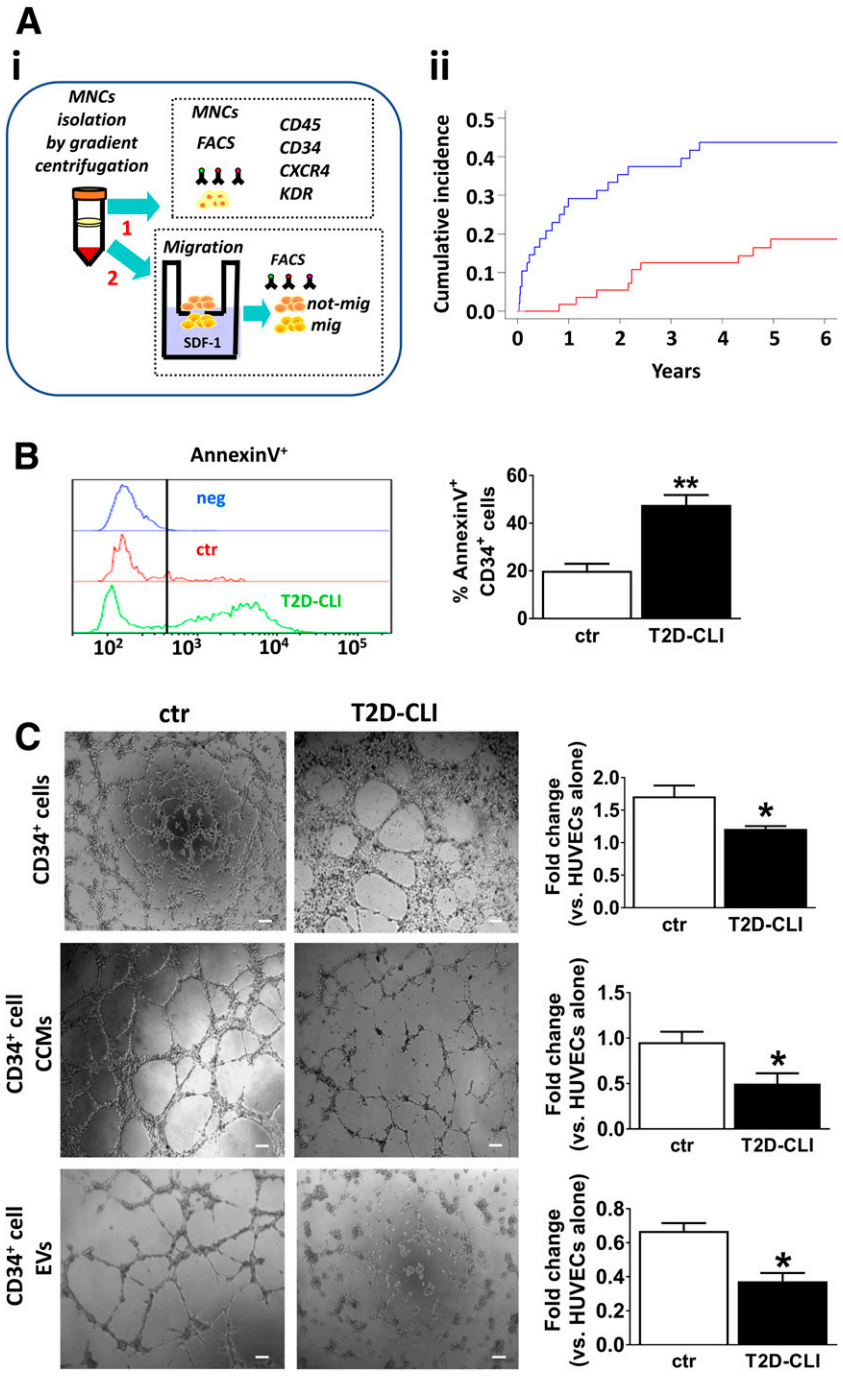

Figure 1—Migration of CD34$^+$ cells toward SDF-1 predicts cardiovascular mortality and is associated with reduced cell viability and angiogenic capacity. *A*: (i) Schematic view of the in vitro migration assay and (ii) cumulative incidence of mortality for cardiovascular causes during the 6-year follow-up in groups categorized according to the median value of CD45^{dim}/CD34$^+$/CXCR4$^+$/KDR$^+$ migrated toward SDF-1. The red line represents the incidence in the group with migration value below the median value, while the blue line indicates the cumulative incidence in the group with migration value equal or above the median. *P* value for the difference between the two curves = 0.0012. *B*: Typical flow cytometry displacement curves and bar graph showing the percent of BM-derived CD34$^+$ cells expressing AnnexinV in control subjects (ctr) and patients with T2D with CLI (T2D-CLI) ($N = 3$ in each group). *C*: Representative microscopy images of the Matrigel assay (scale bars = 50 μm) and bar graphs showing fold changes in the average number of network branches made by HUVECs in the presence or the absence of CD34$^+$ cells (coculture 1:1), CD34$^+$ CCM, or CD34$^+$ cell–derived EVs from control subjects (empty bars, $N = 5$) or patients with T2D-CLI (black bars, $N = 4$). Values are means ± SE; *$P < 0.05$ vs. ctr.

with an optical microscope (Eclipse E800; Nikon) at 40× magnification and quantified by using ImageJ software.

In Vitro Angiogenesis

BM-CD34$^+$ cells, their CCM, or isolated EVs were cocultured with HUVECs (1:1 ratio) on Matrigel (Corning Incorporated Life Sciences) (15).

Statistical Analyses

Continuous variables were expressed as mean ± SD or SE as indicated, tested for normality by the Kolmogorov-Smirnov test, and compared using parametric (*t* test or ANOVA) or nonparametric tests (Wilcoxon or Kruskal-Wallis), as appropriate. Categorical variables were expressed as frequency and percentage and were compared by χ^2 test or Fisher exact test. A *P* value <0.05 was considered statistically significant. SAS (version 9.4), R (version 3.4.4), and GraphPad Prism (version 7) were used for analyses and graphics.

In study 1, cumulative incidences of events were drawn overall and for data stratified by cells (above versus below the median) that significantly differed between participants with or without events. This analysis considered the competitive causes of the event (16); specifically, in the case of cardiovascular death, other causes of death were considered as a competitive event, and vice versa. Comparisons between incidence curves were assessed fitting the proportional subdistribution hazards regression model (17). Time-to-event was defined as the time from revascularization to death (cardiovascular or for other causes). Patients lost to follow-up were excluded from the analyses. The 15th day of a given month and the month of June were imputed if the day or month of follow-up was missing, respectively. Incidence rate and 95% CI at 3 years and 6 years of follow-up were calculated for cardiovascular death and for other causes of death.

To evaluate the association between basal cell counts and migratory activity and risk of death, the event-specific hazard ratio (HR) and 95% CI was calculated. HRs associated with cell migration were evaluated for a 1-year increase, for the presence of a history of coronary artery disease, and for a 0.01-unit increase in the percentage of CD45^{dim}CD34$^+$CXCR4$^+$KDR$^+$ migrated cells toward SDF-1 over total MNCs. All

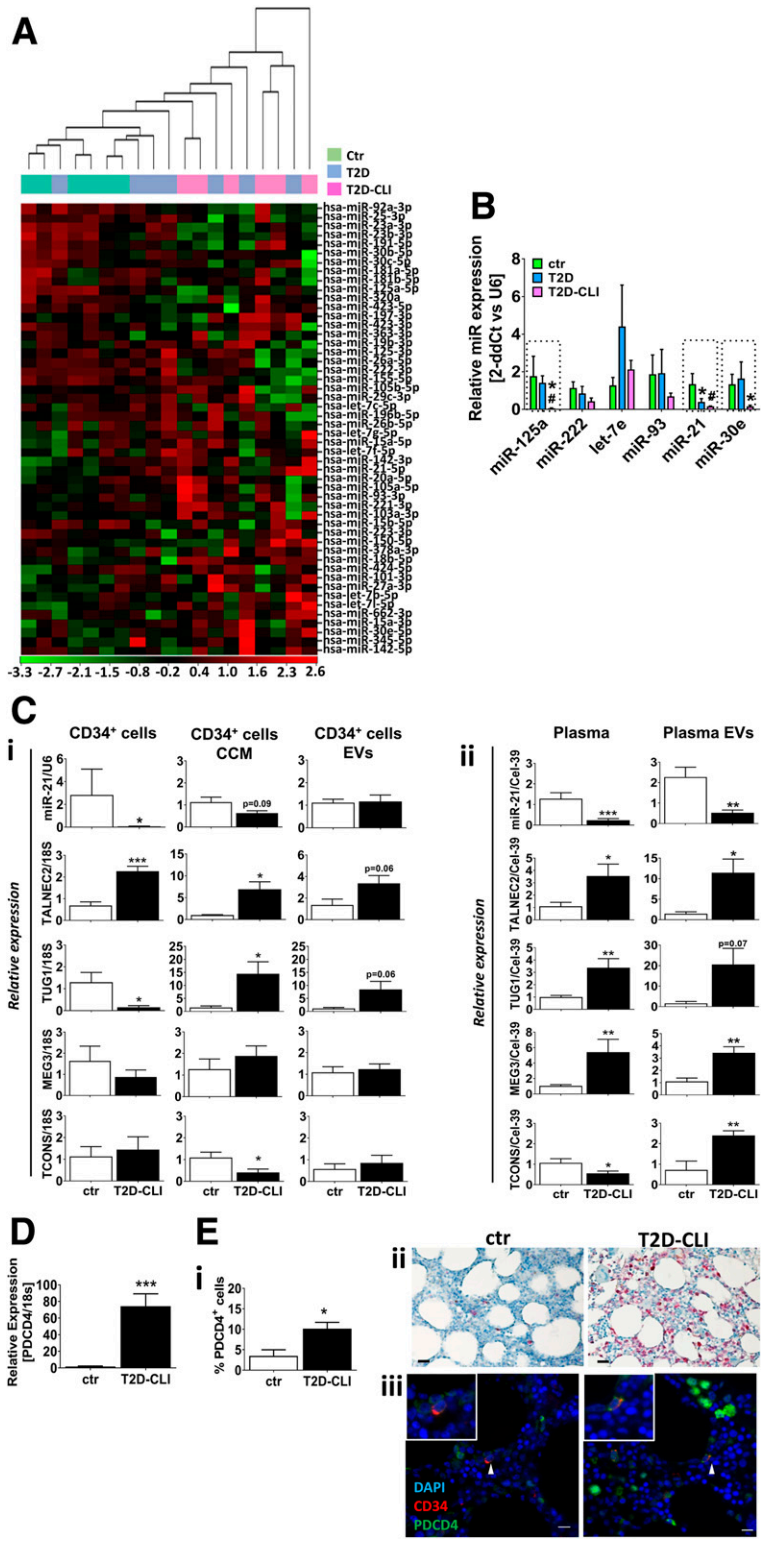

Figure 2—miRNA profiling of BM-derived CD34$^+$ cells unveils the modulation of miRNA-21 and its target PDCD4 in patients with T2D and CLI. *A*: Heat map showing that BM-CD34$^+$ cells isolated from subjects with T2D either uncomplicated (T2D) or complicated by CLI (T2D-CLI) bear a specific miR profile. Quantitative RT-PCR data, $N = 6$ donor/group. *B*: A bar graph showing the average relative expression of a group of six miRs assessed in a validation study on BM-CD34$^+$ cells obtained from donors different from those used in profiling (control subjects [ctr]: $N = 5$, patients with T2D: $N = 4$, patients with T2D-CLI: $N = 4$). Quantitative RT-PCR, $^*P < 0.05$ vs. ctr, $^{\#}P < 0.05$ vs. with T2D. *C*: (i) Relative expression of mature miR-21 and miR-21 sponges in BM-derived CD34$^+$ cells ($N = 4$), CD34$^+$ CCM (ctr: $N = 8$, T2D-CLI: $N = 7$), and isolated EVs (ctr: $N = 8$, T2D-CLI: $N = 7$) from new donors. (ii) Relative expression of mature miR-21 and miR-21 sponges in plasma ($N = 9$–10) and EVs

models were performed for the presence of investigated variable, if dichotomous, and for a 1-unit increase of continuous variables, if not otherwise specified. A multivariable regression model was subsequently implemented, adjusting for prognostic features that were found significantly associated with the event in the univariate analysis.

RESULTS

CD34$^+$ Cell Migration and Cardiovascular Mortality

Supplementary Table 1 illustrates clinical/laboratory data of the 104 T2D-CLI patients who completed the 6-year follow-up.

Three outcomes were considered: no event ($N = 54$), cardiovascular death ($N = 32$), and other causes of death ($N = 18$). Age at recruitment was the only clinical data that differed among the three outcomes ($P = 0.0067$) (Supplementary Table 4). Regarding CD45^{dim}CD34$^+$CXCR4$^+$KDR$^+$ cells, migration toward SDF-1 (experimental setting illustrated in Fig. 1*Ai*) was higher in the cardiovascular death group compared with no event group or the other causes of death group ($P = 0.0312$), whereas there was no difference in PB levels of CD45^{dim}CD34$^+$CXCR4$^+$KDR$^+$ cells or in the migration of total MNCs and CD45^{dim}CD34$^+$CXCR4$^+$KDR$^+$ cells exposed to the SDF-1 vehicle (Supplementary Table 5 and Supplementary Fig. 1).

As shown in Fig. 1*Aii* and Supplementary Table 6, patients with values of SDF-1–migrated cells greater than or equal to the median had higher cumulative incidence of cardiovascular death compared with those with values less than the median ($P = 0.0012$). Cell migration was associated with an increased cardiovascular risk (HR 1.10, 95% CI 1.04–1.17, $P = 0.0005$, data not shown), which was further confirmed by a multivariable Cox analysis simultaneously assessing the effect of age and prevalence of coronary artery disease (Supplementary Table 7).

BM-CD34$^+$ Cell Viability and Angiogenic Activity

To obtain mechanistic insights into the observed association, we studied the functional characteristics of BM-CD34$^+$ cells from a new series of patients with T2D or T2D-CLI and control subjects without diabetes.

In line with previous studies (13), flow cytometry analyses demonstrated that CD34$^+$ cells immune-magnetically sorted from the BM of T2D-CLI patients have a 2.5-fold higher abundance of 7-AAD$^-$/Annexin V$^+$ events compared with controls (Fig. 1*B*).

Moreover, using an in vitro Matrigel assay, we demonstrated that the coculture of HUVECs with T2D-CLI BM-CD34$^+$cells resulted in a lower number of branches compared with the coculture of HUVECs and control BM-CD34$^+$ cells (Fig. 1*C*). A marked decrease in endothelial network formation was also observed when incubating HUVECs with BM-CD34$^+$ cell–derived CCM or EVs from patients with T2D-CLI (Fig. 1*C*). These data demonstrate that BM-CD34$^+$ cells from T2D-CLI patients have reduced viability and can transfer destabilizing signals to endothelial cells through factors secreted as soluble molecules or packaged in EVs.

miR Signature in BM-CD34$^+$ Cells

Diabetes influences the expression of several miRs in hematopoietic cells (11–13). An unbiased miR profiling of CD34$^+$ cells isolated from the BM of control subjects ($N = 6$) and T2D patients with ($N = 6$) or without CLI ($N = 7$) identified a suppressive effect of T2D on the quantity of expressed miRs (Supplementary Fig. 2*A* and *B*), which might be attributable to the downregulation of Dicer (Supplementary Fig. 2*C* and *D*), an endoribonuclease involved in miRNA maturation, as also described by others (18).

Supplementary Table 8 shows that 56 miRs were commonly expressed in the three groups. Moreover, 2 sets of 11 different miRs were shared by control subjects and patients with T2D-CLI or control subjects and patients with T2D, respectively. Of those not shared, 49 were unique to control subjects and 1, namely miR-146a, to T2D-CLI, whereas none was exclusive to T2D. As shown in Supplementary Table 9, 18 miRs were differentially expressed in cells from T2D subjects, with or without CLI, compared with control subjects, with 2 of them, miR-21 and miR-30e, being shared by the two T2D groups. The heatmap diagram in Fig. 2*A* indicates a marked separation of miR expression in patients with T2D-CLI compared with control subjects, while values from patients with T2D were spread between control subjects and patients with T2D-CLI. Among the miRs that showed a differential expression between patients with T2D-CLI and control subjects, we studied a set of six miRs (miR-125a, miR-222, let-7e, miR-93, miR-21, and miR-30e) known to control cell survival, differentiation, hematopoiesis, and angiogenesis (Supplementary Table 10). To validate the profiling results, we performed single PCR analyses for the six miRs of interest on BM-CD34$^+$ cells isolated from a new set of donors (control subjects, $N = 5$; patients with T2D, $N = 4$; patients with T2D-CLI, $N = 4$) using an Applied Biosystem platform and normalizing miR expression to U6snoRNA, which showed a stable expression among the three groups. Three miRs from the set of choice, miR-125a, miR-21, and miR-30e, were significantly modulated in the new cohort (Fig. 2*B*).

Downregulation of miR-21 Associated With Reciprocal Changes in Its Target PDCD4

miR-21, one of the most highly expressed miRs in mammalian cells, is modulated in cardiovascular disease (19–23). However, little is known regarding the expression of miR-21 in hematopoietic progenitor cells. Data of RT-PCR confirmed the downregulation of mature miR-21 in sorted T2D-CLI BM-CD34$^+$ cells (Fig. 2*C*i), whereas the levels of the corresponding pri-miR were similar to controls (data not shown). miR-21 was also found in CD34$^+$ cell–derived CCMs and EVs, but no difference was seen when comparing patients with T2D-CLI and control subjects (Fig. 2*C*i). Interestingly, miR-21 levels were decreased in plasma and EVs isolated from the PB of T2D-CLI patients (Fig. 2*C*ii).

Long ncRNAs can act as miR sponges, thereby interfering with regulation of miR targets. We investigated the expression of several long ncRNAs reportedly implicated miR-21 modulation (24–28). As shown in Fig. 2*C*i, TALNEC2 was upregulated in T2D-CLI BM-CD34$^+$ cells and respective CCM; TUG1 was decreased in cells and increased in the CCM; MEG3 was not altered; and TCONS was downregulated in CCM. These data suggest that TALNEC2 could inhibit miR-21 at intracellular level, and, together with TUG1, at extracellular level. Moreover, all the studied sponges were upregulated either in plasma, EVs, or both, suggesting they may synergize in inhibiting miR-21 in the circulation (Fig. 2*C*ii).

The proapoptotic factor PDCD4 is a validated target of miR-21 (19). In line with the miR-21 downregulation, we found higher *PDCD4* mRNA levels in T2D-CLI BM-CD34$^+$ cells (Fig. 2*D*). Likewise, in situ immunohistochemistry confirmed the higher expression of PDCD4 in the BM (Fig. 2*E*). Altogether, these data point at a novel molecular mechanism involving the downregulation of miR-21 and induction of PDCD4 in T2D-CLI CD34$^+$ cells.

Migration Toward SDF-1 Enriches a Population of CD34$^+$/CXCR$^+$/PDCD4$^+$ Cells

CD34$^+$CXCR4$^+$ cells represented a small fraction (1.5 $\pm$ 0.2%) of the total CD34$^+$ cell population in PB of T2D-CLI patients. PDCD4 was more abundant in the CD34$^+$CXCR4$^+$ (77.9 $\pm$ 0.4%) than in the CD34$^+$CXCR4$^-$ cell fraction (5.8 $\pm$ 0.2%). Moreover, SDF-1–stimulated migration of PB-MNCs resulted in an enrichment of cells expressing both CXCR4 and PDCD4 in the migrated fraction (Supplementary Fig. 3).

Silencing miR-21 in Control BM-CD34$^+$ Cells Recapitulates the Negative Features of T2D-CLI CD34$^+$ Cells

Next, we sought confirmation of a direct link between T2D-CLI–associated miR-21 downregulation and BM-CD34$^+$ cell dysfunction. To this aim, we silenced miR-21 in control BM-CD34$^+$ cells using an anti-miR strategy. The effective miR-21 knockdown (Fig. 3*A*) was associated with *PDCD4* upregulation (Fig. 3*B*) and increased apoptotic events compared with SCR-treated cells (Fig. 3*C*). Moreover, miR-21 silencing conferred anti-angiogenic properties to CD34$^+$ cells as

($N = 4$–5). Quantitative RT-PCR, $^*P < 0.05$, $^*P < 0.01$, and $^{***}P < 0.001$ vs. ctr. *D*: PDCD4 mRNA modulation in T2D-CLI BM-CD34$^+$ cells. Quantitative RT-PCR ($N = 8$), $^*P < 0.05$ vs. ctr. *E*: (i) A bar graph showing the frequency of PDCD4-positive cells over the total number of hematoxylin-positive nuclei in the BM of ctr and T2D-CLI subjects ($N = 3$). $^*P < 0.05$ vs. ctr. Representative microphotographs of BM (ii) using immunohistochemistry (scale bars = 20 μm) and (iii) immunofluorescent microscopy (scale bars = 10 μm). White arrowheads indicate CD34$^+$ cells.

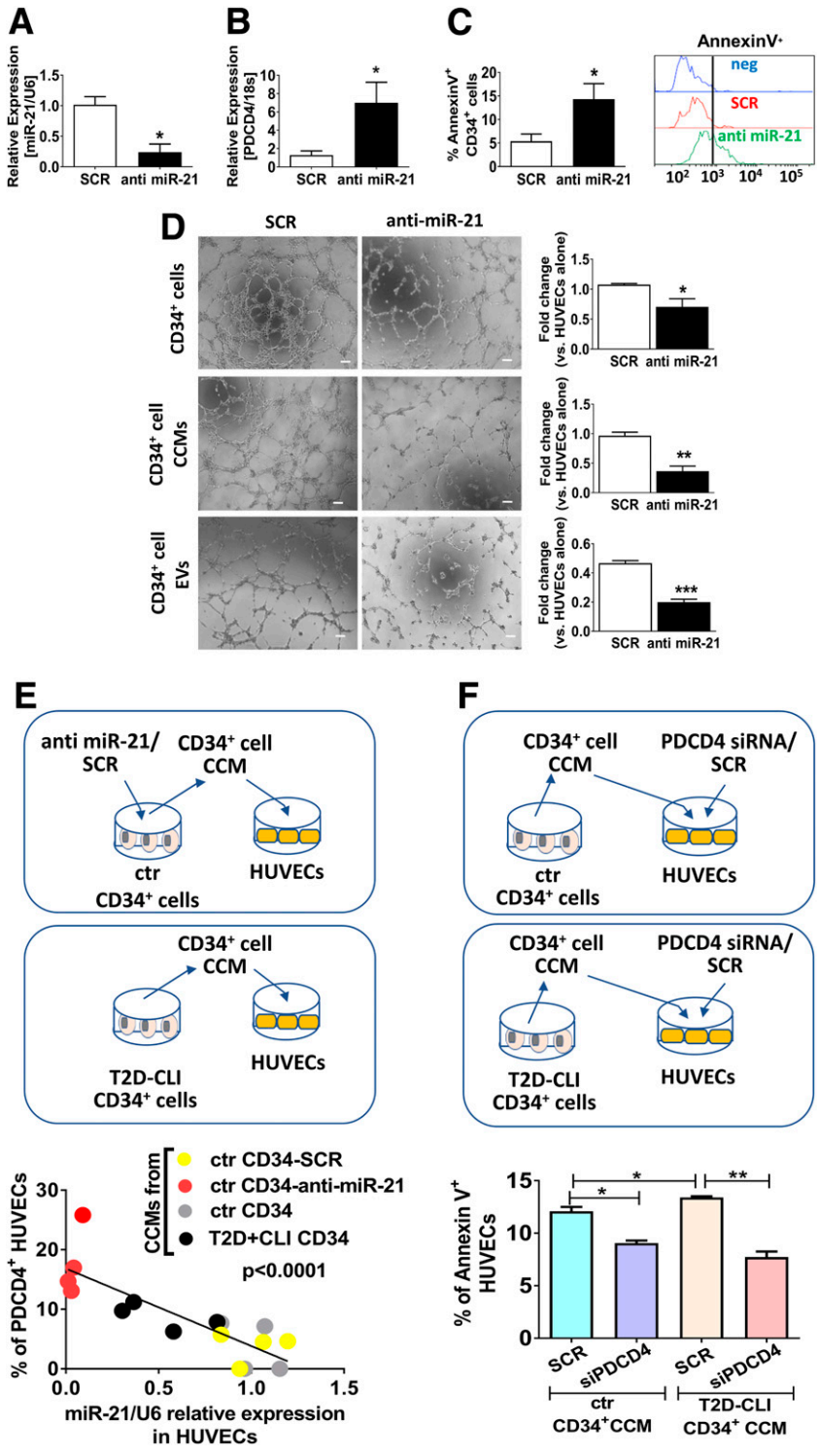

Figure 3—Inhibition of miR-21 in BM-CD34$^+$ cells from control subjects mimics diabetes-associated dysfunction. *A*: Silencing miR-21 in CD34$^+$ cells resulted in miR-21 reduction (RT-PCR, $N = 3$). *B*: Silencing miR-21 in CD34$^+$ cells also resulted in PDCD4 upregulation (RT-PCR, $N = 6$). *$P < 0.05$ vs. SCR. *C*: miR-21 inhibition is associated with increased apoptosis of BM-CD34$^+$ cells, shown as a bar graph of Annexin V$^+$/7AAD$^-$ cells assessed using flow cytometry ($N = 7$). *D*: Antiangiogenic action of miR-21-silenced BM-CD34$^+$ cells ($N = 4$), CCM ($N = 3$), and EVs ($N = 3$). HUVECs networking analysis on Matrigel (scale bars = 50 μm). *E*: A shematic view of the experimental setting (left); a negative correlation between PDCD4 and miR-21 in HUVECs treated with the CCM from CD34$^+$ cells (right). The graph reports data of average PDCD4 protein levels (as percentage of positive HUVECs identified using immunofluorescence microscopy) and average miR-21 expressional levels (by PCR analysis). Colored circles indicate the source of CCMs. *F*: A schematic of the experiment (top); a bar graph shows the percentage of Annexin V$^+$/7AAD$^-$ HUVECs either SCR- or siPDCD4-transfected after treatment with CD34$^+$-CCM (bottom). Flow cytometry analysis, $N = 3$ donors/condition.

well as to the CD34$^+$ cell–derived CCM and EVs (Fig. 3*D*).

Transfer of Proapoptotic miR-21/PDCD4 Signaling to Endothelial Cells

We next assessed if the negative cross-talk between CD34$^+$ cells and endothelial cells involves the direct transfer of miR-21 or PDCD4 or is mediated by associated factors. To this purpose, using a protocol illustrated in Fig. 3*E*, we measured the relative expression of miR-21 and PDCD4 in HUVECs exposed to the CCM from control CD34$^+$ cells (either naive or transfected with anti-miR-21 or SCR) or to the CCM from T2D-CLI CD34$^+$ cells. Interestingly, plotting the expressional values of miR-21 and PDCD4 from the four groups demonstrated an inverse relationship between the miR and its target (Fig. 3*E*). This indicates that modulation of the miR-21/PDCD4 duo in BM-CD34$^+$ cells can induce similar expressional changes in the exposed endothelial cells. Next, employing a protocol illustrated in Fig. 3*F*, we demonstrated that *PDCD4* silencing in HUVECs remarkably reduced the apoptosis caused by the exposure to the CCM from T2D-CLI CD34$^+$ cells (Fig. 3*F*). A dedicated ELISA could not detect PDCD4 in the CD34$^+$ cell–derived CCM. These data suggest that CD34$^+$ cells induce apoptosis in HUVECs through different paracrine mechanisms.

Implication of TUG1 and Oxidative Stress

The presence of miR-21 sponges in the CCM from T2D-CLI CD34$^+$ cells suggested that they could act paracrinally to inhibit miR-21 in endothelial cells. Therefore, we assessed TALNEC2, TUG1, MEG3, and TCONS in HUVECs either naive or exposed to the CCM from CD34$^+$ cells from control or T2D-CLI subjects. Results confirmed the downregulation of miR-21 and the induction of PDCD4 by the T2D-CLI CCM and demonstrated that TUG1 was the only upregulated long ncRNA in conditioned HUVECs (Fig. 4*A*).

Reciprocal interactions exist between long ncRNAs and reactive oxygen species (ROS) production and scavenging (29). Relevant to our study, H_2O_2 and hypoxia reportedly induced TUG1 in cardiomyocytes, thereby increasing ROS production and apoptosis (30). Hence, we hypothesized that oxidative stress could be involved in the transfer of

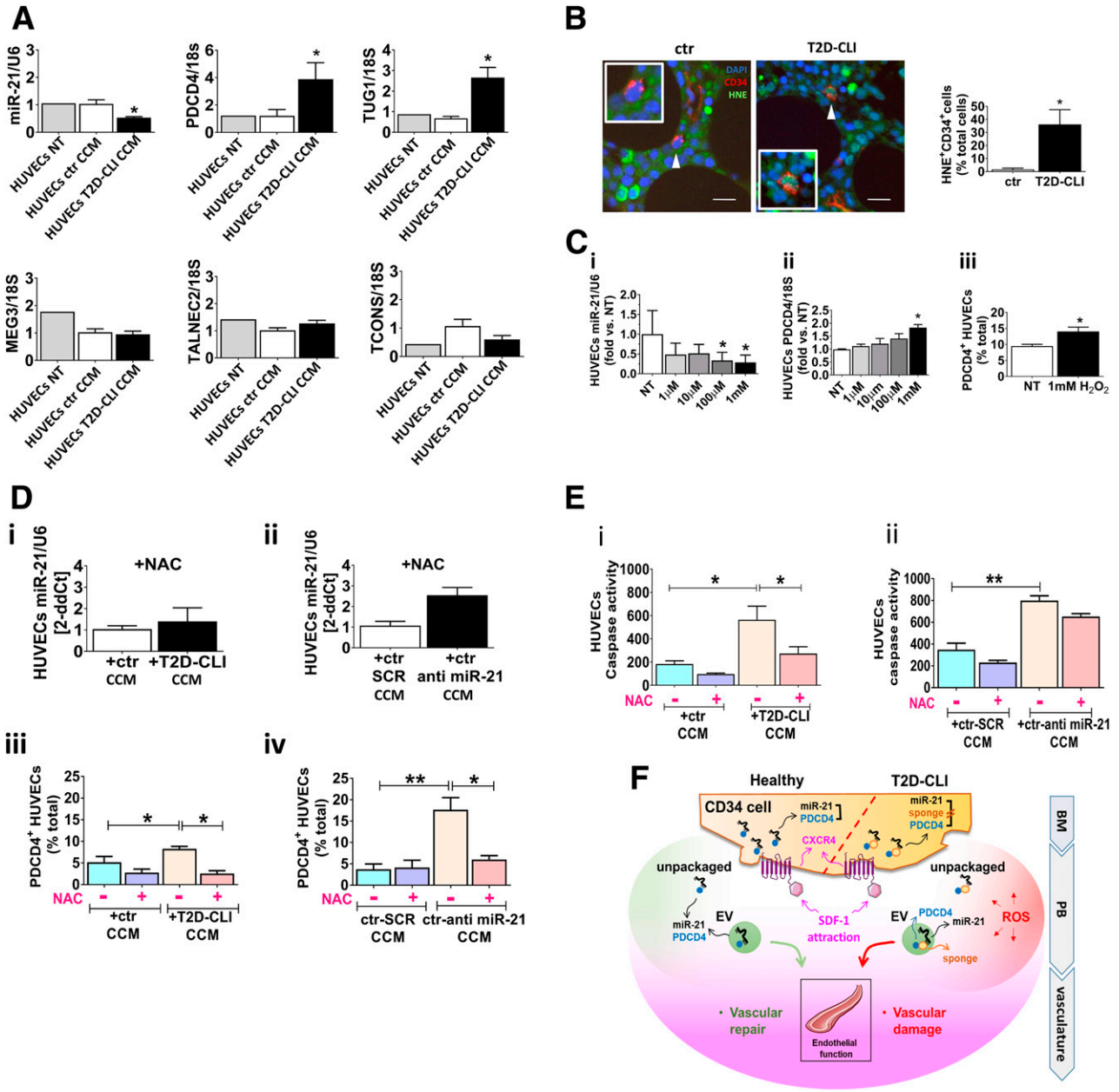

Figure 4—Exposure of endothelial cells to the conditioned medium of CD34$^+$ cells from patients with T2D and CLI induces a modulation of the miR-21/PDCD4 axis through a mechanism involving reactive oxygen species and the miR-21 sponge TUG1. *A*: A bar graph showing the average relative expression of miR-21, PDCD4, and indicated long ncRNA in HUVECs either not treated (NT) or treated with the conditioned media (CCM) from BM-derived CD34$^+$ cells of control subjects (ctr) or T2D-CLI patients (T2D-CLI) ($N = 4$ donors). *$P < 0.05$ vs. ctr CCM. *B*: In situ detection of ROS levels assessed by measuring 4-HNE in BM-CD34$^+$ cells. Representative images of immunofluorescence staining (IF) and a bar graph of average data (ctr: $N = 5$, T2D-CLI: $N = 6$). *$P <$ 0.05. White arrowheads in IF microphotographs indicate CD34$^+$ cells (scale bars = 10 μm). *C*: A bar graph showing the relative expression of (i) miR-21 and (ii) PDCD4 mRNA (RT-PCR, $N = 6$) and (iii) PDCD4 protein (IF, NT: $N = 3$, treated: $N = 5$) in HUVECs exposed to H_2O_2 at the indicated concentrations. *$P < 0.05$ vs. NT. *D*: Antioxidant action of NAC results in the prevention of miR-21 inhibition in HUVECs that were exposed (i) to the CCM of CD34$^+$ cells from patients with T2D-CLI or (ii) to the CCM of miR-21-silenced CD34$^+$ cells from ctr. Bar graphs with average RT-PCR data show that there was no difference with respective CCM from ctr CD34$^+$ cells or CCM from ctr CD34$^+$ cells transfected with SCR siRNA. (iii) The percentage of PDCD4-positive HUVECs exposed to the CCM of CD34$^+$ cells from ctr or T2D-CLI patients with (+) or without (−) NAC. *$P < 0.05$ as indicated by the lines. (iv) The percentage of PDCD4-positive HUVECs exposed to the CCM of ctr CD34$^+$ cells, transfected with either SCR or anti-miR-21, with (+) or without (−) NAC. *$P < 0.05$ and **$P < 0.01$ as indicated by the lines. $N = 4$ in each group for all the experiments. *E*: NAC scavenging of ROS protects HUVECs from CD34-CCM-induced apotosis. Conditions in (i) and (ii) are the same as in *E* (iii) and (iv), respectively. Bar graphs of average caspase 3/7 activity that was measured using ELISA. *$P < 0.05$ and **$P < 0.01$ as indicated by the lines ($N = 3$). *F*: A diagram of the proposed molecular interaction between CD34$^+$ cell and endothelial cells, involving the participation of ROS and miR-21 sponge TUG1. The section of CD34$^+$ cell on the left of the dotted line shows the inhibition of proapoptotic PDCD4 by miR-21 leading to prosurvival signaling to the vascular endothelium. The section of CD34$^+$ cell on the right illustrates the interference of the miR-21 sponge on the inhibitory target, which results in activation of proapoptotic signaling in the vascular endothelium.

proapoptotic signaling to endothelial cells. This was confirmed by the following evidence: *1*) T2D-CLI BM-CD34$^+$ cells showed elevated in situ 4-HNE staining, a marker of oxidative damage and lipid peroxidation (Fig. 4*B*); *2*) treatment of HUVECs with increasing H_2O_2 concentrations induced miR-21 inhibition and PDCD4 upregulation (Fig. 4*C*); and *3*) ROS scavenging with *N*-acetylcysteine (NAC) blocked the miR-21 downregulation in HUVECs exposed to the CCM from T2D-CLI CD34$^+$ cells (Fig. 4*D*i) or to the CCM from anti-miR-21-transfected control CD34$^+$ cells (Fig. 4*D*ii). In parallel, NAC abrogated the induction of PDCD4 by the CCMs (Fig. 4*D*iii and iv). It also counteracted the apoptosis of HUVECs exposed to the CCM from T2D-CLI CD34$^+$ cells (Fig. 4*E*i) but was unable to prevent the apoptosis of HUVECs exposed to the CCM from miR-21-silenced CD34$^+$ cells (Fig. 4*E*ii). These findings indicate that ROS in association with TUG1 is the likely mediator for transmission of an altered miR-21/PDCD4 balance from T2D-CLI CD34$^+$ cells to endothelial cells (Fig. 4*F*). They also point to the possibility that the total disruption of miR-21 impacts on additional proapoptotic inducers that are independent of ROS.

CONCLUSIONS

In an extended follow-up of T2D-CLI patients, CD34$^+$ cell migration maintained a predictive value at 6 years after angioplasty. In these critical patients, CD34 cells responsive to SDF-1 chemoattraction exert negative effects on the vascular endothelium through a mechanism involving miR-21 inhibition and PDCD4 upregulation.

In the high-migratory group, cardiovascular mortality accrued during the first years of follow-up, with the difference versus the low-migratory group remaining unchanged later. Most patients with the highest cardiovascular risk had already died at that stage, resulting in a reduction of the target for prediction. Moreover, mortality for other causes can act as a strong opposer in an elderly population. Nonetheless, the biomarker maintained its validity in a multivariable analysis accounting for the age of participants.

Reduction and dysfunction of stem/progenitor cells is associated with and predicts adverse outcomes of diabetic complications (8). Thus, at first glance, our data appear counterintuitive. We hypothesized that subfractions of BM-CD34$^+$ cells could become antiangiogenic and proapoptotic due to the adverse metabolic milieu they are exposed to in the BM and in circulation. Once they enter the circulation, these cells may convey pathogenic signals to the vascular endothelium, thereby accelerating ischemic complications.

Accumulating evidence indicates that CLI aggravates the remodeling effect of T2D on the BM niche and induces a senescent phenotype in CD34$^+$ cells, which may be, at least in part, attributable to alteration in miR biogenesis, expression, and degradation (13,18). The observed reduction of expressed miRs in BM-CD34$^+$ cells from T2D patients may be attributable to a block in the miR processing, as suggested by Dicer downregulation. Among differentially expressed miRs, we focused on miR-21 because of its involvement in cardiovascular disease (31–34). miR-21 downregulation in T2D-CLI CD34$^+$ cells was associated with upregulation of the programmed cell death protein PDCD4, a validated inhibitory target of miR-21, and with alterations in viability and proangiogenic activity of CD34$^+$ cells. Silencing miR-21 reproduced the same phenotype in CD34$^+$ cells of subjects without diabetes. Moreover, data of an SDF-1 migration assay on T2D-CLI PB-MNCs demonstrated the high coexpression of PDCD4 and CXCR4 within the migrated CD34$^+$ cell fraction. This finding provides a key of interpretation for the link between CD34$^+$CXCR4$^+$ cell migration and cardiovascular death in the follow-up study on T2D-CLI patients.

miR-21 is the most abundant miRNA in macrophages and its downregulation has been associated with induction of atherosclerosis, plaque necrosis, and vascular inflammation (35). Silencing of miR-21 in macrophages increases the expression of mitogen-activated protein kinase kinase 3, thereby leading to the activation of the p38-CHOP and c-Jun N-terminal kinase signaling pathways and triggering macrophage apoptosis (35). Additionally, miR-21–silenced macrophages are unable to remove apoptotic cells, which contributes in delaying the resolution of inflammation (35). The miR-21 inhibitory target PDCD4 acts as a tumor suppressor protein involved in programmed cell death. Recent cardiovascular research has shown that PDCD4 is upregulated in coronary arteries of atherosclerotic rats, where it participates in the formation of coronary plaques, through destabilization of vascular smooth muscle cells and promotion of inflammatory chemokines (36). Nonetheless, the regulation of miR-21/PDCD4 interaction is only partially known. Prostaglandins reportedly act as inducers of miR-21 expression and suppressors of PDCD4 protein, whereas cyclooxygenase 2 inhibitors produce opposite effects (37). Moreover, several long ncRNAs can act as sponges for miR-21 (24–28). For instance, miR-21 is a direct target of MEG3, and in hypoxic vascular cells, MEG3 interferes with miR-21 modulation of PTEN resulting in cell proliferation and migration (27). Likewise, studies on H9c2 cells showed that TALNEC2 modulates miR-21/PDCD4 expression under hypoxia, aggravating its consequences (25). TCONS is an endothelium-associated long ncRNA involved in plaque progression. Binding of miR-21 to TCONS reduces its expression and, for this reason, was proposed as potential treatment to improve endothelial dysfunction and plaque stabilization (28). Finally, TUG1 was proposed to interact miR-21 and to modulate endothelial cell apoptosis (38). Both oxidative stress and ischemia induce the sponging activity of TUG1, thereby stimulating intracellular ROS accumulation and aggravating the ischemic injury (30). Interestingly, we found that the above long ncRNAs were modulated in CD34$^+$ cells and PB of T2D-CLI patients. Moreover, exposure of HUVECs to the CCM of T2D-CLI CD34$^+$ cells induced the expression of TUG1 and PDCD4, while suppressing miR-21. This mechanism may be ROS dependent when considering that the inhibition exerted by NAC resulted in improved cell survival. We propose that CD34$^+$ cells recruited from PB may exert a sponge-dependent inhibition of the interaction between miR-21 and PDCD4, thereby sustaining vascular damage. Elevated PB levels of miR-21 sponges could strengthen this cellular crosstalk.

These findings have clinical and therapeutic implications, but they also raise new questions. Currently, the long-term prognosis of CLI is based on clinical parameters (39). Our study suggests that the assessment of the CD34$^+$ cells profile may help identify high-risk patients for whom more aggressive treatments are necessary. Although more sophisticated than traditional biomarkers, cellular biomarkers can

be very useful in helping us understand the complex interplay among cellular systems in inducing diabetic vascular disease. In this respect, circulating cells offer a more feasible means for molecular profiling than BM cells, also considering the variability in cell composition of different BM sites. This last aspect represents a limitation of our study, as BM samples were obtained from the femoral head or iliac crest aspirates with the intention of not interfering with clinical practice and patient care.

PDCD4 might represent a valuable biomarker and therapeutic target in ischemic disease. The latter assumption is indirectly supported by the established benefit of prostaglandin E1, an inhibitor of PDCD4, in the treatment of limb ischemia. Novel treatments targeting upstream modulators of PDCD4, including miR-21 and related sponges, might be also considered for treatment of CLI. Finally, autologous BM-CD34$^+$ cells are currently used in clinical trials of CLI patients. Our study calls for caution in using CD34$^+$ cells that carry a proapoptotic and antiangiogenic molecular signature, e.g., low miR-21/high PDCD4. New investigation is needed to determine if this signature can be exploited to increase the safety and efficacy of the cell therapy approach.

Acknowledgments. The authors thank Dr. Simona Rodighiero, Imaging Unit of the Department of Experimental Oncology, European Institute of Oncology, Milan, Italy, for the support in the generation of the microscopy data and immunofluorescence data presented herein.

Funding. Funding and financial support was obtained from the Italian Ministry of Health, Ricerca Corrente to the IRCCS MultiMedica, Foundation Cariplo (2016-0922), and a British Heart Foundation program grant. Study 1 was also supported by Diabetic ONLUS Association, section of Treviso.

Duality of Interest. No potential conflicts of interest relevant to this article were reported.

Author Contributions. G.S. and P.M. acquired funding, analyzed data, and wrote the manuscript. E.S. researched data relative to both study 1 and study 2. E.T. performed the statistical analyses for study 1. D.M. isolated cells and performed the in vitro molecular analyses of study 2. O.C. conducted tissue and cells immune characterization. D.F.-M. isolated cells and provided biological samples. F.C. and P.O. provided human BM samples and contributed to the discussion. A.P. acquired funding and contributed to the discussion. A.F., P.M.S., and L.S. were involved in collection of the human BM samples and recording the clinical data. M.S. acquired funding, provided human BM samples, and corrected the manuscript. G.S. and P.M. are the guarantors of this work and, as such, had full access to all the data in the study and take responsibility for the integrity of the data and the accuracy of the data analysis.

Prior Presentation. Parts of this study were presented in abstract form at the Keystone Symposia: Novel Aspects of Bone Biology (E3), Snowbird, UT, 13–16 June 2018 and at the European Society of Cardiology Congress, Paris, France, 31 August to 4 September 2019.

References

1. Welch JS, Ley TJ, Link DC, et al. The origin and evolution of mutations in acute myeloid leukemia. Cell 2012;150:264–278
2. Forsberg LA, Gisselsson D, Dumanski JP. Mosaicism in health and disease - clones picking up speed. Nat Rev Genet 2017;18:128–142
3. Jaiswal S, Fontanillas P, Flannick J, et al. Age-related clonal hematopoiesis associated with adverse outcomes. N Engl J Med 2014;371:2488–2498
4. Jaiswal S, Natarajan P, Silver AJ, et al. Clonal hematopoiesis and risk of atherosclerotic cardiovascular disease. N Engl J Med 2017;377:111–121
5. Albiero M, Ciciliot S, Tedesco S, et al. Diabetes-associated myelopoiesis drives stem cell mobilopathy through an OSM-p66Shc signaling pathway. Diabetes 2019;68:1303–1314
6. Fadini GP, Rigato M, Cappellari R, Bonora BM, Avogaro A. Long-term prediction of cardiovascular outcomes by circulating CD34+ and CD34+ CD133+ stem cells in patients with type 2 diabetes. Diabetes Care 2017;40:125–131
7. Rigato M, Bittante C, Albiero M, Avogaro A, Fadini GP. Circulating progenitor cell count predicts microvascular outcomes in type 2 diabetic patients. J Clin Endocrinol Metab 2015;100:2666–2672
8. Rigato M, Avogaro A, Fadini GP. Levels of circulating progenitor cells, cardiovascular outcomes and death: a meta-analysis of prospective observational studies. Circ Res 2016;118:1930–1939
9. Caballero S, Sengupta N, Afzal A, et al. Ischemic vascular damage can be repaired by healthy, but not diabetic, endothelial progenitor cells. Diabetes 2007;56:960–967
10. Spinetti G, Specchia C, Fortunato O, et al. Migratory activity of circulating mononuclear cells is associated with cardiovascular mortality in type 2 diabetic patients with critical limb ischemia. Diabetes Care 2014;37:1410–1417
11. Spinetti G, Fortunato O, Cordella D, et al. Tissue kallikrein is essential for invasive capacity of circulating proangiogenic cells. Circ Res 2011;108:284–293
12. Spinetti G, Fortunato O, Caporali A, et al. MicroRNA-15a and microRNA-16 impair human circulating proangiogenic cell functions and are increased in the proangiogenic cells and serum of patients with critical limb ischemia. Circ Res 2013;112:335–346
13. Spinetti G, Cordella D, Fortunato O, et al. Global remodeling of the vascular stem cell niche in bone marrow of diabetic patients: implication of the microRNA-155/FOXO3a signaling pathway. Circ Res 2013;112:510–522
14. Ferland-McCollough D, Maselli D, Spinetti G, et al. MCP-1 feedback loop between adipocytes and mesenchymal stromal cells causes fat accumulation and contributes to hematopoietic stem cell rarefaction in the bone marrow of patients with diabetes. Diabetes 2018;67:1380–1394
15. Besnier M, Gasparino S, Vono R, et al. miR-210 enhances the therapeutic potential of bone-marrow-derived circulating proangiogenic cells in the setting of limb ischemia. Mol Ther 2018;26:1694–1705
16. Prentice RL, Kalbfleisch JD, Peterson AV Jr., Flournoy N, Farewell VT, Breslow NE. The analysis of failure times in the presence of competing risks. Biometrics 1978;34:541–554
17. Fine JP and Gray RJ. A proportional hazards model for the subdistribution of a competing risk. J Am Stat Assoc 1999;94:496–509
18. Elgheznawy A, Shi L, Hu J, et al. Dicer cleavage by calpain determines platelet microRNA levels and function in diabetes. Circ Res 2015;117:157–165
19. Cheng Y, Liu X, Zhang S, Lin Y, Yang J, Zhang C. MicroRNA-21 protects against the H(2)O(2)-induced injury on cardiac myocytes via its target gene PDCD4. J Mol Cell Cardiol 2009;47:5–14
20. Gu H, Liu Z, Li Y, et al. Serum-derived extracellular vesicles protect against acute myocardial infarction by regulating miR-21/PDCD4 signaling pathway. Front Physiol 2018;9:348
21. Gu GL, Xu XL, Sun XT, et al. Cardioprotective effect of microRNA-21 in murine myocardial infarction. Cardiovasc Ther 2015;33:109–117
22. Huang W, Tian SS, Hang PZ, Sun C, Guo J, Du ZM. Combination of microRNA-21 and microRNA-146a attenuates cardiac dysfunction and apoptosis during acute myocardial infarction in mice. Mol Ther Nucleic Acids 2016;5:e296
23. Thum T, Gross C, Fiedler J, et al. MicroRNA-21 contributes to myocardial disease by stimulating MAP kinase signalling in fibroblasts. Nature 2008;456:980–984
24. Zhu B, Gong Y, Yan G, et al. Down-regulation of lncRNA MEG3 promotes hypoxia-induced human pulmonary artery smooth muscle cell proliferation and migration via repressing PTEN by sponging miR-21. Biochem Biophys Res Commun 2018;495:2125–2132
25. Hao L, Wang J, Liu N. Long noncoding RNA TALNEC2 regulates myocardial ischemic injury in H9c2 cells by regulating miR-21/PDCD4-medited activation of Wnt/β-catenin pathway. J Cell Biochem 2019;120:12912–12923
26. Li FP, Lin DQ, Gao LY. LncRNA TUG1 promotes proliferation of vascular smooth muscle cell and atherosclerosis through regulating miRNA-21/PTEN axis. Eur Rev Med Pharmacol Sci 2018;22:7439–7447
27. Wu Z, He Y, Li D, et al. Long noncoding RNA MEG3 suppressed endothelial cell proliferation and migration through regulating miR-21. Am J Transl Res 2017;9:3326–3335
28. Halimulati M, Duman B, Nijiati J, Aizezi A. Long noncoding RNA TCONS_00024652 regulates vascular endothelial cell proliferation and angiogenesis via microRNA-21. Exp Ther Med 2018;16:3309–3316
29. Fuschi P, Maimone B, Gaetano C, Martelli F. Noncoding RNAs in the vascular system response to oxidative stress. Antioxid Redox Signal 2019;30:992–1010
30. Su Q, Liu Y, Lv XW, Dai RX, Yang XH, Kong BH. LncRNA TUG1 mediates ischemic myocardial injury by targeting miR-132-3p/HDAC3 axis. Am J Physiol Heart Circ Physiol 2020;318:H332–H344
31. Chan JA, Krichevsky AM, Kosik KS. MicroRNA-21 is an antiapoptotic factor in human glioblastoma cells. Cancer Res 2005;65:6029–6033

32. Kulshreshtha R, Ferracin M, Wojcik SE, et al. A microRNA signature of hypoxia. Mol Cell Biol 2007; 27:1859–1867
33. Liu LZ, Li C, Chen Q, et al. MiR-21 induced angiogenesis through AKT and ERK activation and HIF-1α expression. PLoS One 2011;6:e19139
34. Xu X, Kriegel AJ, Jiao X, et al. miR-21 in ischemia/reperfusion injury: a double-edged sword? Physiol Genomics 2014;46:789–797
35. Canfrán-Duque A, Rotllan N, Zhang X, et al. Macrophage deficiency of miR-21 promotes apoptosis, plaque necrosis, and vascular inflammation during atherogenesis. EMBO Mol Med 2017;9:1244–1262
36. Gao Y, Li H, Zhou Y, Lv H, Chen Y. PDCD4 expression in coronary atherosclerosis rat models and its mechanism. Exp Ther Med 2019;17: 3150–3154
37. Peacock O, Lee AC, Cameron F, et al. Inflammation and MiR-21 pathways functionally interact to downregulate PDCD4 in colorectal cancer. PLoS One 2014;9:e110267
38. Chen C, Cheng G, Yang X, Li C, Shi R, Zhao N. Tanshinol suppresses endothelial cells apoptosis in mice with atherosclerosis via lncRNA TUG1 up-regulating the expression of miR-26a. Am J Transl Res 2016;8:2981–2991
39. Faglia E, Clerici G, Clerissi J, et al. Long-term prognosis of diabetic patients with critical limb ischemia: a population-based cohort study [published correction appears in Diabetes Care 2009;32:1355]. Diabetes Care 2009;32: 822–827